Nonlinear Tracking Control of a Human Limb via Neuromuscular Electrical Stimulation

K. Stegath[1], N. Sharma[1], C. M. Gregory[2], and W. E. Dixon[1]

Abstract— A nonlinear control method is developed in this paper that uses neuromuscular electrical stimulation to control the human quadriceps femoris muscle undergoing non-isometric contractions. The objective of the controller is to position the lower limb of a human along a time-varying trajectory or a desired setpoint. The developed controller does not require a muscle model and can be proven to yield asymptotic stability for a nonlinear muscle model in the presence of bounded nonlinear disturbances. Performance of the controller is illustrated in the provided experimental results.

I. INTRODUCTION

Neuromuscular electrical stimulation (NMES) is the application of a potential field across a muscle via internally or externally placed electrodes in order to produce a desired muscle contraction. NMES is a prescribed treatment for a number of neurological dysfunctions. Because of the potential for improvements in daily activities by people with movement disorders such as stroke and spinal cord injuries, the development of NMES as a neuroprosthesis has grown rapidly [1]. However, the application and growth of NMES technologies have been stymied by several technical challenges related to the design of an automatic stimulation strategy. Specifically, due to a variety of uncertainties in muscle physiology (e.g., temperature, pH, and architecture), predicting the exact contraction force exerted by the muscle is difficult. One cause of this difficulty is that there is an unknown mapping between the generated muscle force and stimulation parameters. There are additional problems with delivering consistent stimulation energy to the muscle due to electrode placement, percentage of subcutaneous body fat, muscle fatigue, as well as overall body hydration. There are also time delays between the delivery of the stimulation signal and the contraction of the muscle.

Given the uncertainties in the structure of the muscle model and the parametric uncertainty for specific muscles, some investigators have explored various linear PID-based pure feedback methods (c.f. [2]–[6] and the references within). Typically, these approaches have only been empirically investigated and no analytical stability analysis has been developed that provides an indication of the performance, robustness or stability of these control methods.

Some recent studies (e.g., see [7]) also point to evidence that suggests that linear control methods do not yield acceptable performance in practice. The development of a stability analysis for previous PID-based NMES controllers has been evasive because of the fact that the governing equations for a muscle contraction/limb motion are nonlinear with unstructured uncertainties. Some efforts have focused on analytical control development for linear controllers (e.g., [5], [8], [9]); however, the governing equations are typically linearized to accommodate a gain scheduling or linear optimal controller approach.

Motivated by the lack of control development for PID-based feedback methods, significant research efforts have focused on the use of neural network-based controllers (c.f. [10]–[18] and the references within). Nonlinear neural network methods provided a framework that allowed the performance, robustness, and stability of the developed NMES controllers to be investigated without linearization assumptions. However, all of the previous neural network-based NMES controllers are limited to a uniformly ultimately bounded result because of the inevitable residual nonlinear function approximation error. Additionally, neural networks may exhibit performance degradation during the transient phase while the estimates update.

Recently, a new continuous feedback method (coined RISE for Robust Integral of the Sign of the Error in [19], [20]) has been developed that was proven to yield asymptotic tracking of nonlinear systems with unstructured uncertainty and bounded additive disturbances. The contribution of this paper is to illustrate how the RISE controller can be applied for NMES systems. The muscle model considered in this paper is developed and then rewritten in a form that adheres to previous RISE-based Lyapunov stability analyses. The performance of the nonlinear controller is experimentally verified for both the tracking and regulation of a human leg shank by applying the controller as a voltage potential across external electrodes attached to the distal-medial and proximal-lateral portion of the quadriceps femoris muscle group. The RISE controller is implemented by a voltage modulation scheme with a fixed frequency and a fixed pulse width. Other modulation strategies (e.g., frequency or pulse-width modulation) could have also been implemented (and applied to other skeletal muscle groups) without loss of generality. For these initial results, the regulation experiment indicates that the desired knee joint angle can be regulated within $0.5°$ of error, and the tracking experiment can be controlled within $3.5°$ of steady-state error. Future research will focus on including physiological muscle dynamics in

Fig. 1. Diagram of leg extension objective.

the control structure through adaptive feedforward terms.

II. MUSCLE ACTIVATION AND LIMB MODEL

The total knee-joint dynamics can be modeled as [5]

$$M_I + M_e + M_g + M_v + \tau_d = \tau. \tag{1}$$

In (1), $M_I(\ddot{q}) \in \mathbb{R}$ denotes the inertial effects of the shank-foot complex about the knee-joint, $M_e(q) \in \mathbb{R}$ denotes the elastic effects due to joint stiffness, $M_g(q) \in \mathbb{R}$ denotes the gravitational component, $M_v(\dot{q}) \in \mathbb{R}$ denotes the viscous effects due to damping in the musculotendon complex [21], $\tau_d(t) \in \mathbb{R}$ represents unknown unmodelled bounded disturbances (e.g., fatigue, signal and response delays, unmodelled phenomena), and $\tau(t) \in \mathbb{R}$ denotes the torque produced at the knee joint.

The inertial and gravitational effects in (1) can be modelled as

$$M_I(\ddot{q}(t)) = J\ddot{q}(t), \qquad M_g(q(t)) = -mgl\sin(q(t)),$$

where $q(t)$, $\dot{q}(t)$, $\ddot{q}(t) \in \mathbb{R}$ denote the angular position, velocity, and acceleration of the lower shank about the knee-joint, respectively (see Fig. 1), $J \in \mathbb{R}$ denotes the unknown inertia of the combined shank and foot, $m \in \mathbb{R}$ denotes the unknown combined mass of the shank and foot, $l \in \mathbb{R}$ is the unknown distance between the knee-joint and the lumped center of mass of the shank and foot, and $g \in \mathbb{R}$ denotes the gravitational acceleration. The elastic effects are modelled on the empirical findings by Ferrarin and Pedotti in [21] as

$$M_e(q) = -k_1(\exp(-k_2 q(t)))(q(t) - k_3), \tag{2}$$

where k_1, k_2, $k_3 \in \mathbb{R}$ are unknown positive coefficients. As shown in [5], the viscous moment $M_v(\dot{q})$ can be modelled as

$$M_v(\dot{q}(t)) = B_1 \tanh(-B_2 \dot{q}(t)) - B_3 \dot{q}(t), \tag{3}$$

where B_1, B_2, and $B_3 \in \mathbb{R}$ are unknown positive constants.

The torque produced about the knee is controlled through muscle forces that are elicited by NMES. For simplicity (and without loss of generality), the development in this paper focuses on producing knee torque through forces, denoted by $F(t) \in \mathbb{R}$, generated by electrical stimulation of the quadriceps (i.e., we do not consider antagonistic muscle forces). The knee torque is related to the quadriceps force as

$$\tau(t) = \zeta(q(t))F(t), \tag{4}$$

where $\zeta(q(t)) \in \mathbb{R}$ denotes a positive moment arm that changes with the extension and flexion of the leg as shown in studies by [22] and [23]. As indicated in [22], the moment arm $\zeta(q(t))$ has unique values for a given range of motion, while in [23], the moment arm's unique values are obtained for the entire range of motion.

The muscle force $F(t)$ is generated by the available actin and myosin filament binding sites in the muscle fibers. The voltage applied to the muscle alters the calcium ion concentration which influences the actin-myosin binding. The relationship between the muscle force and the applied voltage is denoted by the unknown function $\eta(t) \in \mathbb{R}$ as

$$F(t) = \eta(t)V(t), \tag{5}$$

where $V(t) \in \mathbb{R}$ is the voltage applied to the quadriceps muscle by electrical stimulation. While exact force versus voltage models are debatable and contain parametric uncertainty, the generally accepted empirical relationship between the applied voltage (or similarly, current, frequency [24], [25], or pulse width) is well established.

The following property and assumption have been exploited in subsequent control development.

Property 1: The moment arm $\zeta(q)$ is a continuously differentiable, non zero, positive, monotonic, and bounded function [23], and its first time derivative is bounded. The empirical data [24], [25] indicates the function $\eta(t)$ is a continuously differentiable, non-zero, positive, monotonic, and bounded function, and its first time derivative is bounded.

Assumption 1: The unknown disturbance $\tau_d(t)$ is bounded and its first and second time derivatives exist and are bounded.

Assumption 2: The auxiliary function $\Omega(q, t) \in \mathbb{R}$ defined as the product of $\zeta(q)$ and $\eta(t)$ is continuous, positive, monotonic, and bounded function.

III. CONTROL DEVELOPMENT

The objective in this paper is to develop a NMES controller to produce a knee torque trajectory that will enable a human shank to track a desired trajectory, denoted by $q_d(t) \in \mathbb{R}$. Without loss of generality, the developed controller is applicable to different stimulation protocols (i.e., voltage, frequency, or pulse width modulation). To quantify the objective, a position tracking error, denoted by $e_1(t) \in \mathbb{R}$, is

$$e_1(t) = q_d(t) - q(t), \tag{6}$$

where $q_d(t)$ is an a priori trajectory which is designed such that $q_d(t)$, $q_d^i(t) \in \mathcal{L}_\infty$, where $q_d^i(t)$ denotes the ith derivative for $i = 1, 2, 3, 4$. To facilitate the subsequent analysis, filtered tracking errors, denoted by $e_2(t)$ and $r(t) \in \mathbb{R}$, are defined as

$$e_2(t) = \dot{e}_1(t) + \alpha_1 e_1(t), \tag{7}$$

$$r(t) = \dot{e}_2(t) + \alpha_2 e_2(t), \tag{8}$$

where α_1, $\alpha_2 \in \mathbb{R}$ denote positive constants. The filtered tracking error $r(t)$ is introduced to facilitate the closed-loop error system development and stability analysis but

is not used in the controller because of a dependence on acceleration measurements.

After multiplying (8) by J and utilizing the expressions in (1) and (4) – (7), the following expression can be obtained:

$$Jr = W - \Omega V + \tau_d, \qquad (9)$$

where $W(\dot{e}_1, e_2, t) \in \mathbb{R}$ is an auxiliary signal defined as

$$W = J(\ddot{q}_d + \alpha_1 \dot{e}_1 + \alpha_2 e_2) + M_e + M_g + M_v, \qquad (10)$$

and the continuous, positive, monotonic, and bounded (see assumption 2) auxiliary function $\Omega(q, t) \in \mathbb{R}$ is defined as

$$\Omega = \zeta \eta. \qquad (11)$$

After multiplying (9) by $\Omega^{-1}(q, t) \in \mathbb{R}$, the following expression is obtained:

$$J_\Omega r = W_\Omega - V + \tau_{d\Omega}, \qquad (12)$$

where $J_\Omega(q, t) \in \mathbb{R}$, $W_\Omega(\dot{e}_1, e_2, t) \in \mathbb{R}$, and $\tau_{d\Omega}(q, t) \in \mathbb{R}$ are defined as

$$J_\Omega = \Omega^{-1} J, \qquad W_\Omega = \Omega^{-1} W, \qquad \tau_{d\Omega} = \Omega^{-1} \tau_d.$$

To facilitate the subsequent stability analysis, the open-loop error system for (12) can be determined as

$$J_\Omega \dot{r} = -\frac{1}{2} \dot{J}_\Omega r + N - \dot{V} - e_2, \qquad (13)$$

where $N(e_1, e_2, r, t) \in \mathbb{R}$ denotes the unmeasurable auxiliary term

$$N = \dot{W}_\Omega + e_2 - \frac{1}{2} \dot{J}_\Omega r + \dot{\tau}_{d\Omega}(q, t). \qquad (14)$$

To further facilitate the analysis, another unmeasurable auxiliary term, $N_d(q_d, \dot{q}_d, \ddot{q}_d, \dddot{q}_d, t) \in \mathbb{R}$, is defined as

$$\begin{aligned} N_d = \; & \dot{J}_\Omega(q_d) \ddot{q}_d + J_\Omega(q_d) \dddot{q}_d + \dot{M}_e(q_d) \\ & + \dot{M}_g(q_d) + \dot{M}_v(q_d) + \dot{\tau}_{d\Omega}(q_d, t) \end{aligned} \qquad (15)$$

After adding and subtracting (15) to (13), the open-loop error system can be expressed as

$$J_\Omega \dot{r} = -\dot{V} - e_2 + \tilde{N} + N_d, \qquad (16)$$

where the unmeasurable auxiliary term $\tilde{N}(e_1, e_2, r, t) \in \mathbb{R}$ is defined as

$$\tilde{N}(t) = N - N_d, \qquad (17)$$

Using [26], the Mean Value Theorem is applied to develop the following upper bound

$$\left\| \tilde{N} \right\| \leq \rho(\|z\|) \|z\|, \qquad (18)$$

where $z(t) \in \mathbb{R}^3$ is defined as

$$z(t) \triangleq [e_1^T \; e_2^T \; r^T]^T. \qquad (19)$$

Based on (15), and the fact that $q_d(t)$, $q_d^i(t) \in \mathcal{L}_\infty \; \forall \; i = 1, 2, 3, 4$, the following inequalities can be developed

$$\|N_d\| \leq \zeta_{N_d} \qquad \left\| \dot{N}_d \right\| \leq \zeta_{\dot{N}_d}, \qquad (20)$$

where ζ_{N_d} and $\zeta_{\dot{N}_d} \in \mathbb{R}$ are known positive constants.

The developed open-loop error system in (16) is now similar to the open-loop error system in [19], [20], [27], [28]. Based on the dynamics given in equations (1) – (5) the following RISE feedback controller $V(t)$ is employed as a means to achieve the tracking objective:

$$\begin{aligned} V(t) \triangleq \; & (k_s + 1)e_2(t) - (k_s + 1)e_2(t_0) \\ & + \int_{t_0}^t [(k_s + 1)\alpha_2 e_2(\tau) + \beta \, sgn(e_2(\tau))] d\tau, \end{aligned} \qquad (21)$$

where k_s, $\beta \in \mathbb{R}$ denote positive constant adjustable control gains, and $sgn(\cdot)$ denotes the signum function.

Theorem 1: The controller given in (21) ensures that all system signals are bounded under closed-loop operation. The position tracking error is regulated in the sense that

$$\|e_1(t)\| \to 0 \qquad \text{as} \;\; t \to \infty, \qquad (22)$$

and the controller yields a semi-global stability result provided the control gain k_s, introduced in (21) is selected sufficiently large, and β is selected according to the following sufficient condition:

$$\beta > \left(\zeta_{N_d} + \frac{1}{\alpha_2} \zeta_{\dot{N}_d} \right), \qquad (23)$$

where ζ_{N_d} and $\zeta_{\dot{N}_d}$ are known positive constants.

The stability analysis and complete development of the RISE method can be found in [19], [20], [27], [28].

IV. Experimental Results

Experiments were performed using the RISE controller given in (21). The voltage controller was implemented through an amplitude modulation scheme composed of a variable amplitude positive square wave with a fixed pulse width of $100 \; \mu \sec$ and fixed frequency of 100 Hz. This modulation scheme was arbitrarily chosen and may result in higher fatigue during subject trials compared to other modulation schemes that use lower frequencies. In the future experiments lower frequency will be used to reduce muscle fatigue effects. The following results indicate that the RISE algorithm was able to minimize the knee angle error while dynamically tracking a desired trajectory.

A. Experimental Testbed

A testbed has been constructed at the University of Florida for NMES studies. The testbed shown in Fig.2 consists of a custom computer controlled stimulation circuit and a modified leg extension machine (LEM). The LEM was modified to include optical encoders. The LEM allows seating adjustments to ensure the rotation of the knee is about the encoder axis. For the experiment a 4.5 kg (10 lb.) load was attached to the weight bar of the LEM, and a mechanical stop was used to prevent hyperextension.

A custom stimulation circuit was interfaced with a ServoToGo data acquisition card. The data acquisition was performed at 1000 Hz and consisted of a single encoder whose output was used to determine the knee angle, and two digital-to-analog signals were used as input to the custom stimulation circuitry that produces a $100 \; \mu \sec$ positive

Fig. 2.   Expermental testbed: Dual leg curl and extension machine.

square pulse between $3 - 1000$ Hz with a voltage output between $1 - 100$ volts peak. The I/O card is contained in a Pentium IV PC hosting the real-time operating system QNX. The RISE algorithm was implemented in C++, and the resulting real-time executable was accessed through the QMotor 3.0 Graphical User Interface [29].

In the experiment, bipolar self-adhesive neuromuscular stimulation electrodes were placed over the distal-medial and proximal-lateral portion of the quadriceps femoris muscle group and connected to the custom stimulation circuitry. Prior to participating in the study, written informed consent was obtained from all subjects, as approved by the Institutional Review Board at the University of Florida. Test subject A was a healthy 25 year old male, and test subject B was a healthy 24 year old male. Each test subject was instructed to relax as much as possible and to allow the stimulation to control the limb motion (i.e., the subjects were not supposed to influence the leg motion voluntarily).

To determine bounds on the test subject's response to stimulation, a calibration protocol was performed to determine appropriate upper and lower stimulation bounds. Specifically, an initial stimulation voltage was chosen that would generate a knee joint angle of $25°$. The pulse width was set at 100 $\mu \sec$ and delivered at 100 Hz. Stimulation voltage was linearly increased at the rate of 2 volts per second until the knee joint angle reached $45°$, at which point the voltage would linearly decrease. This ad-hoc strategy provides some indication of the muscle response to stimulation for the different subjects so that the voltage levels could be maintained within safe regions of operation.

B. Regulation Results

For the regulation test, the desired knee angle shown in Fig. 3 increases from $0°$ to $45°$ in 2 seconds, in contrast to simply assigning a set-point of $45°$, for comfort and safety of the study participants. Fig. 3 indicates the desired knee joint angle (long dashed line) and the actual knee joint angle (solid line). A detail of the error in Fig. 4 shows that after 3 seconds the knee joint angle was within $4°$, and after 3.8 seconds when the error reached steady state it never exceeded

$0.5°$. After 8 seconds the knee joint angle was approximately $44.7°$. The RMS and steady state RMS errors were obtained as $7.62°$ and $0.38°$, respectively. The corresponding output voltage computed by the RISE method is shown in Fig. 5.
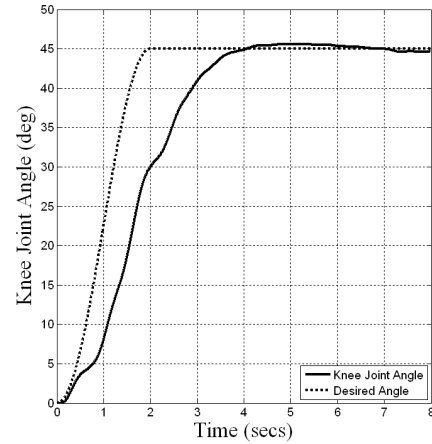
Fig. 3.   Regulation of knee joint angle using the RISE controller.
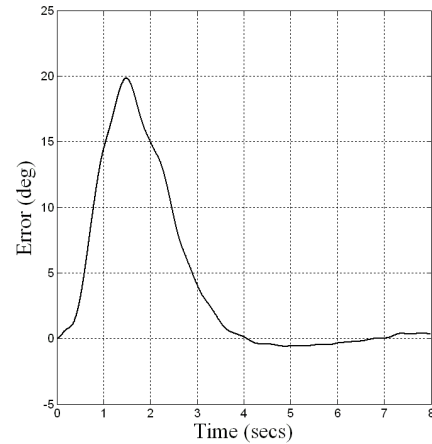
Fig. 4.   Regulation error of knee joint angle (desired angle minus actual angle).

C. Tracking Results

The sinusoidal tracking profile in Fig. 6 was programmed for a minimum angle of $20°$ and a maximum of $45°$. To ensure a smooth (and comfortable) stimulation behavior, two sinusoidal equations were used:

$$q_{d_1}(t) = \frac{\theta_d}{2} + \frac{\theta_d}{2}\left(\sin(\omega t + \frac{3}{2}\pi)\right), \qquad (24)$$

$$q_{d_2}(t) = \left(\frac{\theta_d}{2} - \frac{\theta_m}{2}\right) + \qquad (25)$$

$$\left(\frac{\theta_d}{2} - \frac{\theta_m}{2}\right)\left(\sin(\omega t + \frac{3}{2}\pi)\right) + \theta_m,$$
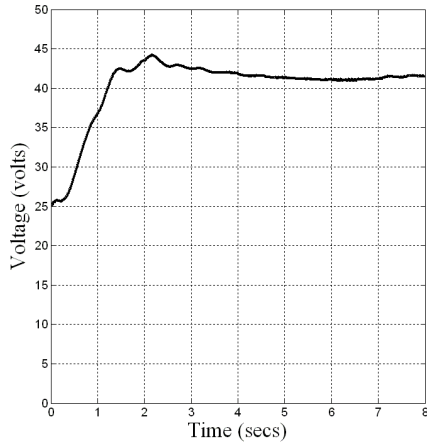
Fig. 5.   RISE voltage during regulation of leg.

where θ_m denotes the minimum knee joint angle, θ_d represents the maximum knee joint angle, and ω denotes the angular frequency with a 4 second period. The desired trajectory in (24) was used until $q_{d_1}(t) = \theta_d$, and then the desired trajectory was changed to $q_{d_2}(t)$ in (25).
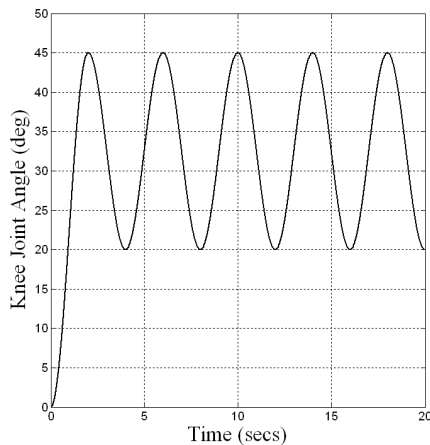
Fig. 6.   Desired tracking profile extended to 20 seconds.

The results of the tracking experiment are shown in Fig. 7. The figure shows the desired knee angle (long dashed line) and the actual knee joint angle (solid line).The plot of the error (Fig. 8) shows a maximum transient error of 17.3° at 1 second which corresponds to the point of maximum velocity. After 1 second the error decreases until approximately 2 seconds when the error reaches steady-state, never exceeding 3.5°. The RMS and steady state RMS errors were obtained as 3.56° and 1.50°, respectively. The corresponding output voltage computed by the RISE method is shown in Fig. 9.

V.   DISCUSSION

A RISE nonlinear control algorithm was applied to NMES to elicit non-isometric contractions of the human quadriceps
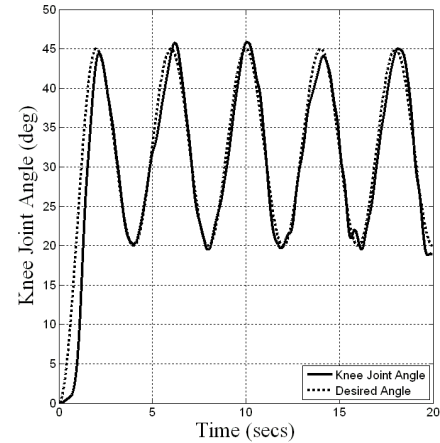
Fig. 7.   Knee joint tracking using the RISE controller.
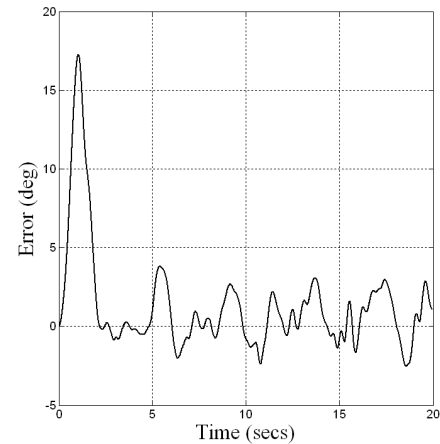
Fig. 8.   Tracking error of knee joint angle (desired angle minus actual angle).

muscle. Two experiments were performed to determine the performance of the RISE control method. The results from both experiments were promising. Specifically, the experimental results indicated that with no muscle model (and only voltage amplitude modulation), the RISE algorithm could determine the appropriate stimulation voltage for both regulation and tracking. The RISE algorithm obtained a regulation error of less than 0.5° and a tracking error of approximately 3.5°.

The primary objective of the first experiment was regulating the knee joint to a desired final angle (45°). The experiment showed a well behaved transient, where within three seconds the error was within 4°. After 3.8 seconds the error never exceeded 0.5°.

The objective for the second experiment required the knee joint to track a desired sinusoidal trajectory with a period of four-seconds. The experiment showed that at the point of maximum velocity (one-second), the controller had a transient error of 17.3°. After approximately 2-seconds (the
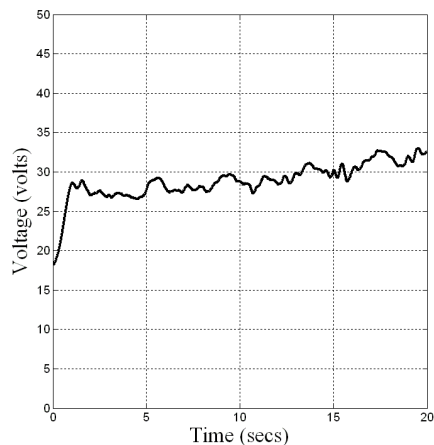
Fig. 9. RISE voltage during knee joint tracking.

point where the velocity is zero) the knee joint tracking error never exceeded $3.5°$.

Future efforts will focus on implementing different modulation methods, stimulating for functional tasks, tracking sinusoidal profile with varying time periods and larger range of motion, examining fatigue induced by the RISE controller, comparing the RISE control results with other NMES methods, and experimental trials on more volunteers, potentially including persons with neurological disorders.

References

[1] P. H. Peckham and D. B. Gray, "Functional neuromuscular stimulation," *J. Rehab. Research Dev.*, vol. 33, pp. 9–11, 1996.

[2] J. J. Abbas and H. J. Chizeck, "Feedback control of coronal plane hip angle in paraplegic subjects using functional neuromuscular stimulation," *IEEE Trans. Biomed Eng.*, vol. 38, no. 7, pp. 687–698, 1991.

[3] N. Lan, P. E. Crago, and H. J. Chizeck, "Control of end-point forces of a multijoint limb by functional neuromuscular stimulation," *IEEE Trans. Biomed. Eng.*, vol. 38, no. 10, pp. 953–965, 1991.

[4] ——, "Feedback control methods for task regulation by electrical stimulation of muscles," *IEEE Trans. Biomed. Eng.*, vol. 38, no. 12, pp. 1213–1223, 1991.

[5] T. Schauer, N. O. Negard, F. Previdi, K. J. Hunt, M. H. Fraser, E. Ferchland, and J. Raisch, "Online identification and nonlinear control of the electrically stimulated quadriceps muscle," *Control Engineering Practice*, vol. 13, pp. 1207–1219, 2005.

[6] K. Stegath, N. Sharma, C. M. Gregory, and W. E. Dixon, "An extremum seeking method for non-isometric neuromuscular electrical stimulation," in *IEEE Int. Conf. Syst., Man, Cybern.*, 2007, pp. 2528–2532.

[7] M. Ferrarin, E. Pavan, R. Spadone, R. Cardini, and C. Frigo, "Standing up exerciser based on functional electrical stimulation and body weight relief," *Medical and Biological Engineering and Computing*, vol. 40, no. 3, pp. 282–289, 2002.

[8] G. Khang and F. E. Zajac, "Paraplegic standing controlled by functional neuromuscular stimulation: Part I - computer model and control-system design," *IEEE Trans. Biomed. Eng.*, vol. 36, no. 9, pp. 873–884, 1989.

[9] F. Previdi, M. Ferrarin, S. Savaresi, and S. Bittanti, "Gain scheduling control of functional electrical stimulation for assisted standing up and sitting down in paraplegia: a simulation study," *Int. J.of Adapt. Control*, vol. 19, pp. 327–338, 2005.

[10] H. Kordylewski and D. Graupe, "Control of neuromuscular stimulation for ambulation by complete paraplegics via artificial neural networks," *Neurol Res.*, vol. 23, no. 5, pp. 472–481, 2001.

[11] J. A. Riess and J. J. Abbas, "Adaptive neural network control of cyclic movements using functional neuromuscular stimulation," *IEEE Trans. Rehab. Eng.*, vol. 8, pp. 42–52, 2000.

[12] E. C. Stites and J. J. Abbas, "Sensitivity and versatility of an adaptive system for controlling cyclic movements using functional neuromuscular stimulation," *IEEE Trans. Biomed. Eng.*, vol. 47, pp. 1287–1292, 2000.

[13] K. Y. Tong and M. H. Granat, "Gait-control system for functional electrical stimulation using neural networks," *Med. Bio. Eng. Comput.*, vol. 37, pp. 35–41, 1999.

[14] F. Sepulveda, M. H. Granat, and A. Cliquet, "Two artificial neural systems for generation of gait swing by means of neuromuscular electrical stimulation," *Med. Eng. Phys.*, vol. 19, pp. 21–28, 1997.

[15] F. Sepulveda, *Computer Techniques in Medical and Biotechnology Systems*. Kluwer Academic Pub., Amsterdam, 2003.

[16] D. G. Zhang and K. Y. Zhu, "Simulation study of fes-assisted standing up with neural network control," in *IEMBS 26th Annual International IEEE Conf. Engineering in Medicine and Biology Society*, vol. 6, 2004, pp. 4118–4121.

[17] J. P. Giuffrida and P. E. Crago, "Functional restoration of elbow extension after spinal-cord injury using a neural network-based synergistic fes controller," *IEEE Trans. Neural Syst. Rehabil. Eng.*, vol. 13, no. 2, pp. 147–152, 2005.

[18] Y. Chen, W. Chen, C. Hsiao, T. Kuo, and J. Lai, "Development of the FES system with neural network + PID controller for the stroke," in *IEEE International Symposium on Circuits and Systems*, vol. 5, 2005, pp. 5119–5121.

[19] P. M. Patre, W. MacKunis, C. Makkar, and W. E. Dixon, "Asymptotic tracking for systems with structured and unstructured uncertainties," *IEEE T. Contr. Syst. T.*, vol. 16, no. 2, pp. 373–379, 2008.

[20] ——, "Asymptotic tracking for systems with structured and unstructured uncertainties," in *IEEE Conference on Decision and Control*, 2006, pp. 441–446.

[21] M. Ferrarin and A. Pedotti, "The relationship between electrical stimulus and joint torque: [a] dynamic model," *IEEE Trans. Rehabil. Eng.*, vol. 8, no. 3, pp. 342–352, 2000.

[22] J. L. Krevolin, M. G. Pandy, and J. C. Pearce, "Moment arm of the patellar tendon in the human knee," *J. Biomech.*, vol. 37, pp. 785–788, 2004.

[23] W. L. Buford, Jr., F. M. Ivey, Jr., J. D. Malone, R. M. Patterson, G. L. Peare, D. K. Nguyen, and A. A. Stewart, "Muscle balance at the knee - moment arms for the normal knee and the ACL - minus knee," *IEEE Trans. Rehabil. Eng*, vol. 5, no. 4, pp. 367–379, 1997.

[24] R. Nathan and M. Tavi, "The influence of stimulation pulse frequency on the generation of joint moments in the upper limb," *IEEE Trans. Biomed. Eng.*, vol. 37, pp. 317–322, 1990.

[25] T. Watanabe, R. Futami, N. Hoshimiya, and Y. Handa, "An approach to a muscle model with a stimulus frequency-force relationship for FES applications," *IEEE Trans. Rehab. Eng.*, vol. 7, No. 1, pp. 12–17, 1999.

[26] V. I. Utkin, *Sliding Modes in Control and Optimization*. New York: Springer-Verlag, 1992.

[27] B. Xian, D. M. Dawson, M. S. de Queiroz, and J. Chen, "A continuous asymptotic tracking control strategy for uncertain multi-input nonlinear systems," *IEEE Trans. Autom. Control*, vol. 49, no. 7, pp. 1206–1211, 2004.

[28] C. Makkar, G. Hu, W. G. Sawyer, and W. E. Dixon, "Lyapunov-based tracking control in the presence of uncertain nonlinear parameterizable friction," *IEEE Trans. Autom. Control*, vol. 52, no. 10, pp. 1988–1994, 2007.

[29] M. Loffler, N. Costescu, and D. Dawson, "Qmotor 3.0 and the qmotor robotic toolkit - an advanced pc-based real-time control platform," *IEEE Control Syst. Mag.*, vol. 22, no. 3, pp. 12–26, 2002.